International Journal of Engineering and Information Systems (IJEAIS)
ISSN: 2643-640X
Vol. 5 Issue 12, December - 2021, Pages:113-122

Flyback Converter Matlab/Simulink Design with Fuzzy Logic Based Control Method

Osman Zenk [1,2] and Birol Ertuğral [1]

[1]Physics, Graduate School of Natural and Applied Sciences, Giresun University, Giresun, Turkey
[2]NYC Bike Rental Corp., New York City, USA
osmanzenk28@gmail.com
[1]Department of Physics, Faculty of Arts and Sciences, Giresun University, Giresun, Turkey
birol.ertugral@giresun.edu.tr

Abstract— *One of the first methods that come to mind in DC power conversion applications is that a Flyback type structure from DC converters is simple to install, the circuit cost is lower than other converter types, and it can give more than one output isolated by source. In addition, flyback converters, which can produce high output voltages, are widely used in switching power supplies, due to their high efficiency. These converters are highly preferred for low power applications. In this study, the Flyback converter was analyzed and its mathematical equations were obtained, its design was made according to the given parameters, and the results were simulated with a Matlab/Simulink based graphic design.*

Keywords— Switched power supplies, DC converters, Flyback converters, Fuzzy Logic controller.

1. INTRODUCTION

Harmful emissions from oil-derived fuels and the phenomenon of global warming have brought renewable and clean energy sources to the fore. It has an important place among renewable energy sources that have no carbon-derived emission, no moving parts, and a modular structure [1]. In recent years, many countries have been rapidly expanding their renewable source energy production systems with increasing incentives [2-3]. According to the 2019 report of the International Energy Agency's (IEA) renewable energies program, its share in global electricity production has reached 23.2% [4]. For a sustainable energy system for humanity, wind energy production methods based on renewable green energy sources [5-6], photovoltaic-based energy production methods [7-8], dam or canal-based hydraulic power plants [9-10], energy production methods with biogas [11-13], geothermal based energy production methods [14] are very important. Many DC converter topologies are available for switching power supplies [15-21]. One of the simplest topologies among the isolated DC converter designs is the flyback converter. The absence of coils in the filter circuit at the output of the circuit, the use of only a transformer as a magnetic element, and the use of only one semiconductor switch make the flyback converter effective [22]. In addition, high output voltage and multiple outputs are the advantages of this flyback converter [23].For these reasons, flyback converters have become the most widely used da-da converters among switch-mode power supplies [24].

2. FLYBACK CONVERTER DESIGN

The logic of energizing the windings in flyback converters is such that while current passes from the polarity in the primary, no current flows from the other or in case of more than one output. Therefore, a transformer movement does not occur. Accordingly, when the switch S in the circuit given in Figure 1 turns on, the Vi source voltage is applied to the primary winding. Due to the reverse polarity of the secondary winding with respect to the primary winding, the diode D is also reverse polarized and therefore no current flows from the secondary [24].

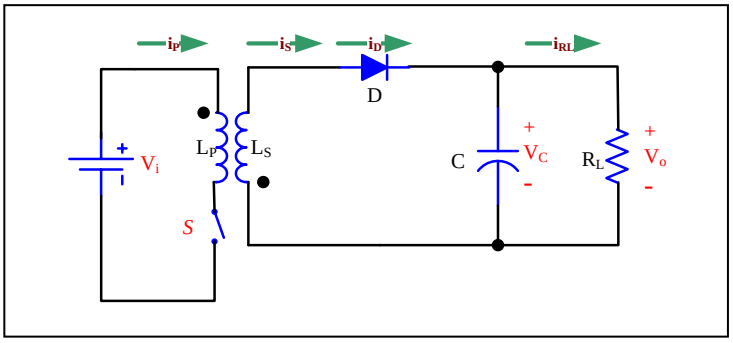

Fig. 1. *Circuit model of a flyback converter*

As seen in Figure 2-a, the current to the load is provided by the energy stored in the capacitor C. Since there is a constant voltage across the Lp terminals, the increase in primary current will be linear. When the S switch is turned off, the energy stored in the air gap

and magnetic core is transmitted to the load via the Ls coil as seen in Figure 2-b. Since there is a constant voltage across the L_S terminals, the current decreases linearly. The energy stored in the air gap is given in Equation (1) from the primary inductance and primary current.

$$E = \frac{L_p I_P^2}{2} \quad (1)$$

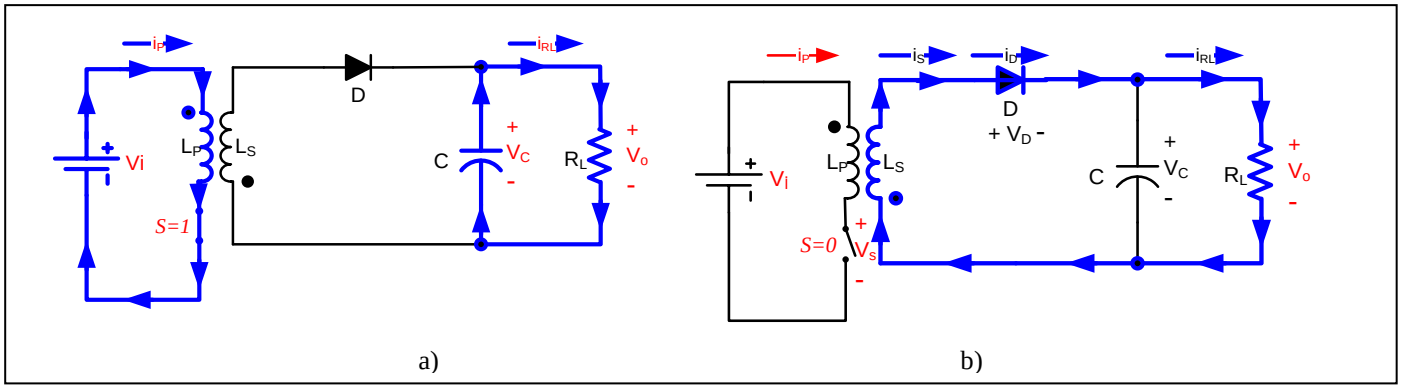

Fig. 2. *Flyback converter circuit operating modes; a) S switch on status b) S switch off status*

As can be seen from Figure 3, in the discontinuous state, the secondary current drops to zero and stays at zero for a certain period of time, before the switch switches to the next conduction state. The sum of the tone and t_{off} times of the key is approximately 80% of the period. The remaining 20% time is called dead time (T_d). In the steady state, there is no T_d. The secondary current does not drop to zero until the next conduction state. The secondary current does not drop to zero until the next transmission state. It is shown in 2 equations that the mean voltage drop across the coil or transformer winding at steady state is equal to zero. The definitions here are; V_i: Input voltage, V_o : Output voltage, t_{on} : Transmission time of semiconductor, t_{off} : Plugging time of semiconductor, V_d : Conduction voltage drop of diode, V_{SW} : Transmission voltage drop of semiconductor switch, n : Transformer conversion ratio.

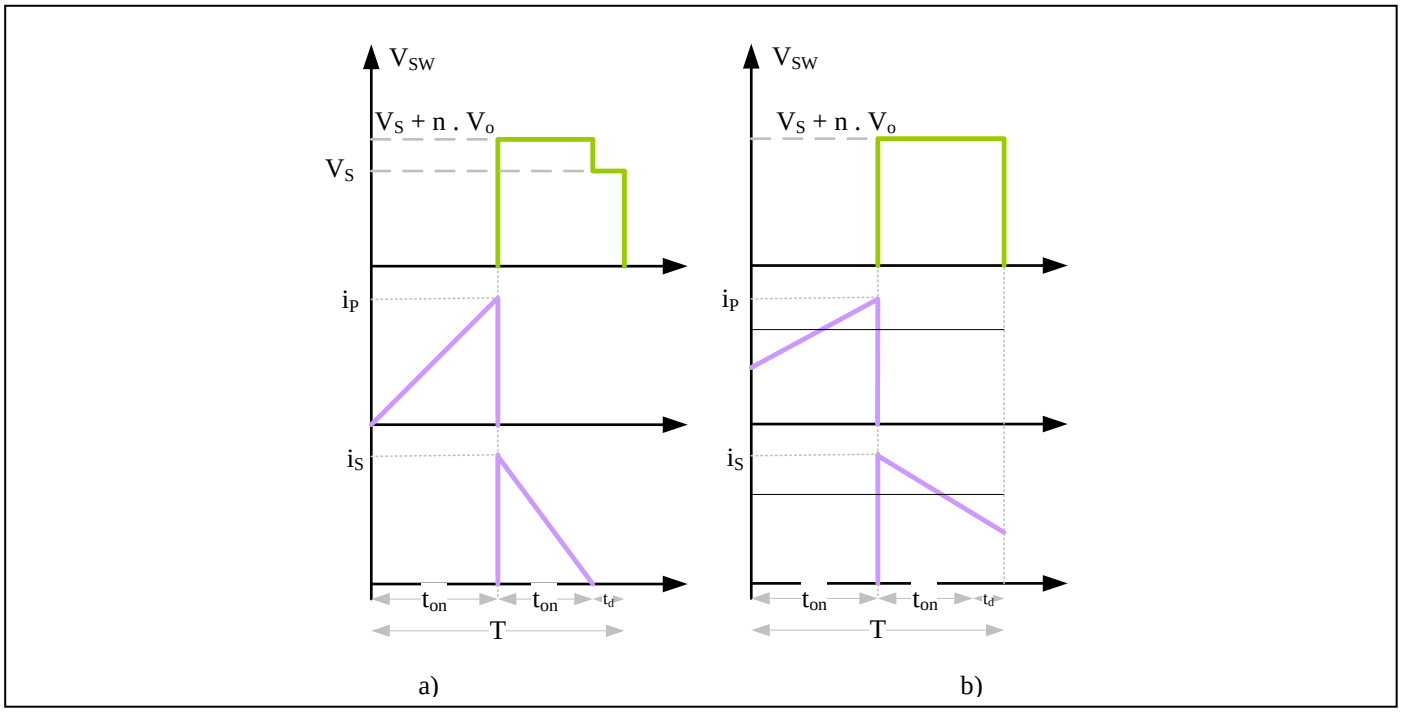

Fig. 3. *Figure 3. a) Discontinuous operating state characteristics, b) Continuous operating state characteristics*

$$(V_i - V_s)T_{on} = (V_o + V_d)\frac{L_P I_P^2}{2} T_{off} a \quad (2)$$

$$T = T_{off} + T_{on} + T_d \quad (3)$$

$$T_{on} = \frac{(V_{out} + V_d)Ta}{(V_{in} + V_s) + (V_{out} + V_d)a} \quad (4)$$

Since the values outside the input voltage are constant in equation (4), the maximum value of the switching time is obtained with the smallest input voltage.

$$T_{on_{\max}} = \frac{(V_{out} + V_d)Ta}{(V_{in_{\min}} + V_s) + (V_{out} + V_d)a} \quad (5)$$

The primary current will increase linearly as the switch has a constant voltage on the primary coil in the transmission state. The current reaches its maximum value, the largest transmission time reaches t_{onmax}. It should be noted that the largest transmission time is possible at the smallest input voltage. According to this, the maximum prime r current I_{pmax} value is given in equation (6).

$$I_{p_{\max}} = \frac{(V_{in_{\max}} + V_s)T_{on_{\max}}}{L_P} \quad (6)$$

Here, L_p is the primary inductance. This current value is stored in the primary winding (in the magnetic core and air gap) for transfer to the secondary winding; When equality (6) is replaced in equality (7), input power equality (8) is obtained.

$$P_{in} = \frac{L_P + I_{P\max}^2}{2T} \quad (7)$$

$$P_{in} = \frac{[V_{in_{\min}} + T_{on\,mac}]}{2TL_P} \quad (8)$$

3. FUZZY LOGIC CONTROLLER DESIGN FOR MATLAB / SIMULINK ENVIRONMENT

In many applications, it is possible to see that membership functions with triangular, trapezoidal, gaussian, sigmoid and sinusoid structures are used. In the modeling made here, triangular membership functions given by the equation (9) are used as in the previous section. In the Simulink environment, x_1, x_2, x_3 are the parameters that represent the exact number whose membership degree will be determined, and the location of the triangle membership function in the relevant definite space. Here x_2 is the exact value that corresponds to the vertex of the triangle, x_1 is the exact value representing the location of the edge on the left side of the vertex, and x_3 is the exact number representing the location of the edge on the right side of the vertex. The fuzzy conclusion mechanism is represented by the verbal expression of equation (10). The conjunction "and" here corresponds to the "min" comparison operator [25-26].

$$\mu(x) = \max\left[\min\left(\frac{x - x_1}{x_1 - x_2}, \frac{x_3 - x}{x_3 - x_2}\right), 0\right] \quad (9)$$

$$\Delta u_R(k) = \frac{\sum_{i=7,8,12,13} \mu_{Ri}(uV_R)\Delta U_R(Ri)}{\sum_{i=1}^{4} \mu_i(uV_R)} \quad (10)$$

If e is A and de is B then du is C (11)

A, B and C parameters correspond to N, S and P fuzzy subsets. The expression given in Equation (11) (If e is A and de is B) represents the partial input space. Therefore, the required weight coefficient for each rule is determined by taking the minimums of the membership values from the input space. In this expression, e is A and is B part are expressions representing blurring. Therefore, the expression (e is A and de is B) represents both the blurring and the determination of the necessary weighting coefficient for the

relevant rule. Output ends shown as mu1, mu2, …mu9 in Figure 4 are the weight coefficient of the fuzzy set corresponding to each output defined in the du output space in the 9-rule FLC [27]. It is multiplied by the exact number with the maximum membership in the numerator of the central method of the areas given by equation (5).

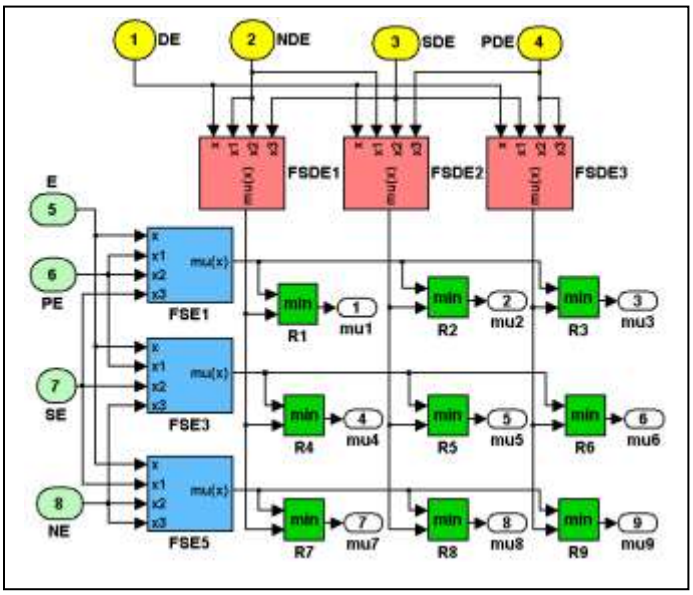

Fig. 4. *Matlab/Simulink model of the statement If e is A and de is B then du is C.*

The clarification method given by Equation (5), the sum of the products in the denominator according to the center of the fields, must be divided by the sum of the membership degrees representing the rule weight coefficients. This process can be performed as shown in Figure 5.

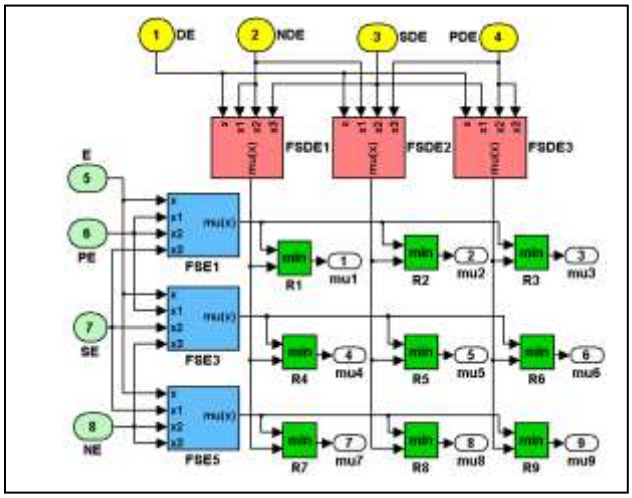

Fig. 5. *Clarification process.*

The block named Blurring given in Figure 4 is a sub-block representing the operations performed with Figure 5, and in the block named Fuzzy Rules, e and de are multiplied by du. The fact that the design is in the form of nested sub-blocks will not only save space, but also reduce complexity. According to the design logic of FLC systems, it is possible to perform the error input directly or by processing the feedback and reference data in the block. It can be done in a block in order to determine the boundaries of the membership functions that will enable the FLC work [28-31].

4. SYSTEM SIMULATION AND EXPLANATIONS

The model of the Fuzzy logic based controller (FLC) and Flyback converter connected system for the proposed designed MATLAB/Simulink environment is given in Figure 6.

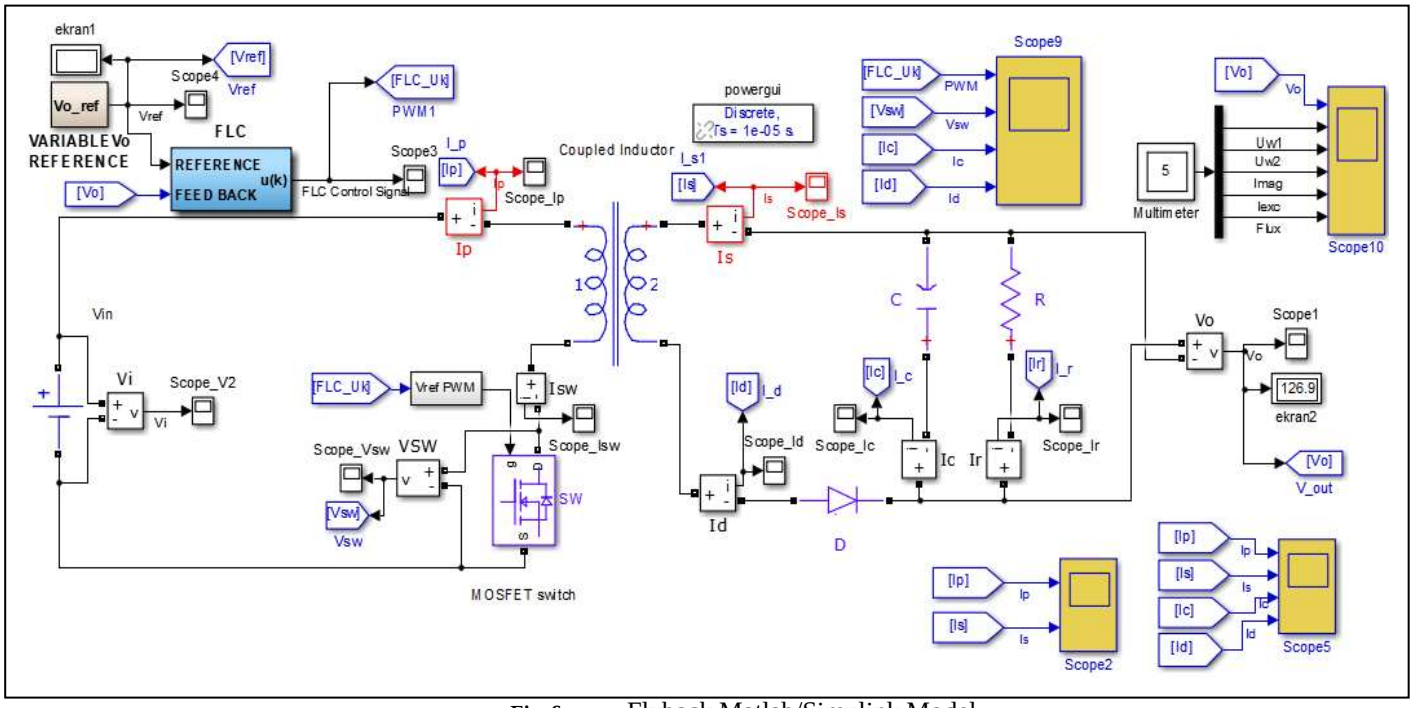

Fig. 6. Flyback Matlab/Simulink Model

Circuit parameters of the designed system are given in Table-1. An application scenario has been prepared so that the system can generate large output voltages with a small DC input voltage of 10V. The system input voltage is connected to the primary input of the coupling inductor. The output end of the primary winding is connected to the MOSFET switch. For the controlled operation of the system, the output voltage is planned to work according to a desired scenario.

Table 1: Battery Pack Parameters

Parameter	Value
Nominal power and frequency [Pn(VA) fn(Hz)]	[1000 $100x10^3$]
Winding 1 and 2 Voltages[V1(Vrms) V2(Vrms)]	[500 500]
Magnetization resistance and inductance [Rm(ohm) Lm(H)]	[10e3 1e-3]
MOSFET resistance Ron (Ohms)	0,1
MOSFET Internal diode resistance Rd (Ohms)	0,01
Diode Resistance Ron (Ohms)	0,001
Diode Forward voltage Vf (V)	0,8 V
Capacitance (F)	$100x10^{-6}$
Resistance (Ohms)	$10x10^3$
Simulation type, simulation solver type, sample time (s)	Discrete, Tustin,$1x10^{-5}$

In Figure 7-a), an image of the output voltage is given for a time of 5 seconds. The fuzzy logic-based controller block (FLC), prepared for the control of the designed flyback inverter system, is shown in blue in the main system. The FLC processes the error signal, which is the difference between a randomly generated, time-varying reference and the voltage signal generated at the output. The u(k) control signals of the FLC, which produce a fast output voltage change, are brought to the appropriate electrical amplitude in the PWM block

for the MOSFET switch to operate. Thus, the primary of the magnetic coupling creates the necessary electrical impulse signals for the secondary winding in order to generate the output voltage. The output voltage (Vo) change signal produced by the flyback converter system, which is approximately similar to the reference voltage (Vref) signal given for the desired output voltage change from the FLC controlling the single switch in the system, is given in Figure 7-b). The signs are generally quite similar to each other, with the differences being related to the simulation time being only 5 seconds. The amount of exceeding the fluctuation level in the output signal produced is at an acceptable level.

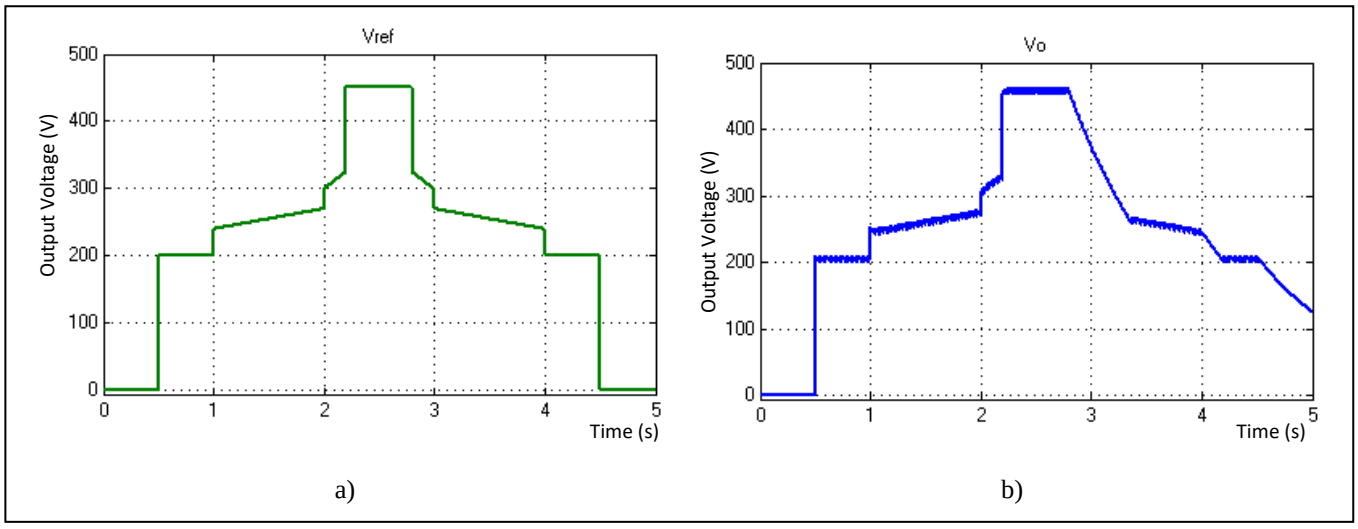

Fig. 7. a) The reference voltage (Vref) sign given for the desired output voltage change from the FLC controller, b) the output voltage (Vo) change sign produced by the flyback converter system.

Figure 8-a) shows the FLC controller output signal series and Figure 8-b) shows the variation of the switch voltage with respect to time.Figure-9 shows the graphs of the change of the main branch currents (primary, secondary, capacitor and diode currents) in the flyback converter system according to the simulation time.

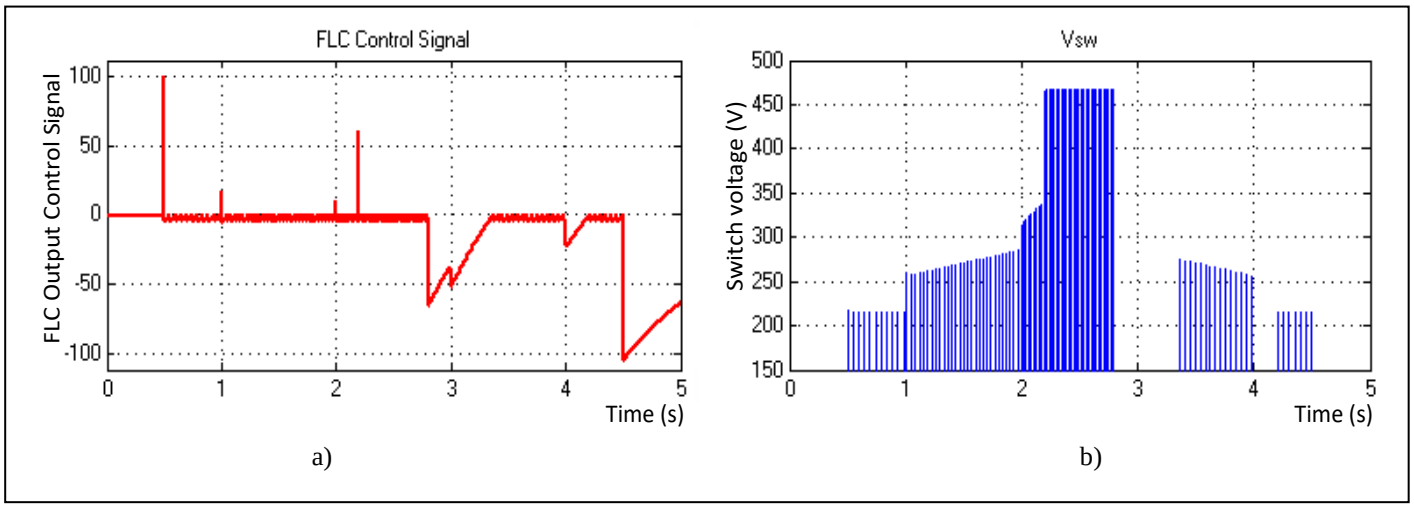

Fig. 8. a) FLC controller output signal series, b) switch voltage (V).

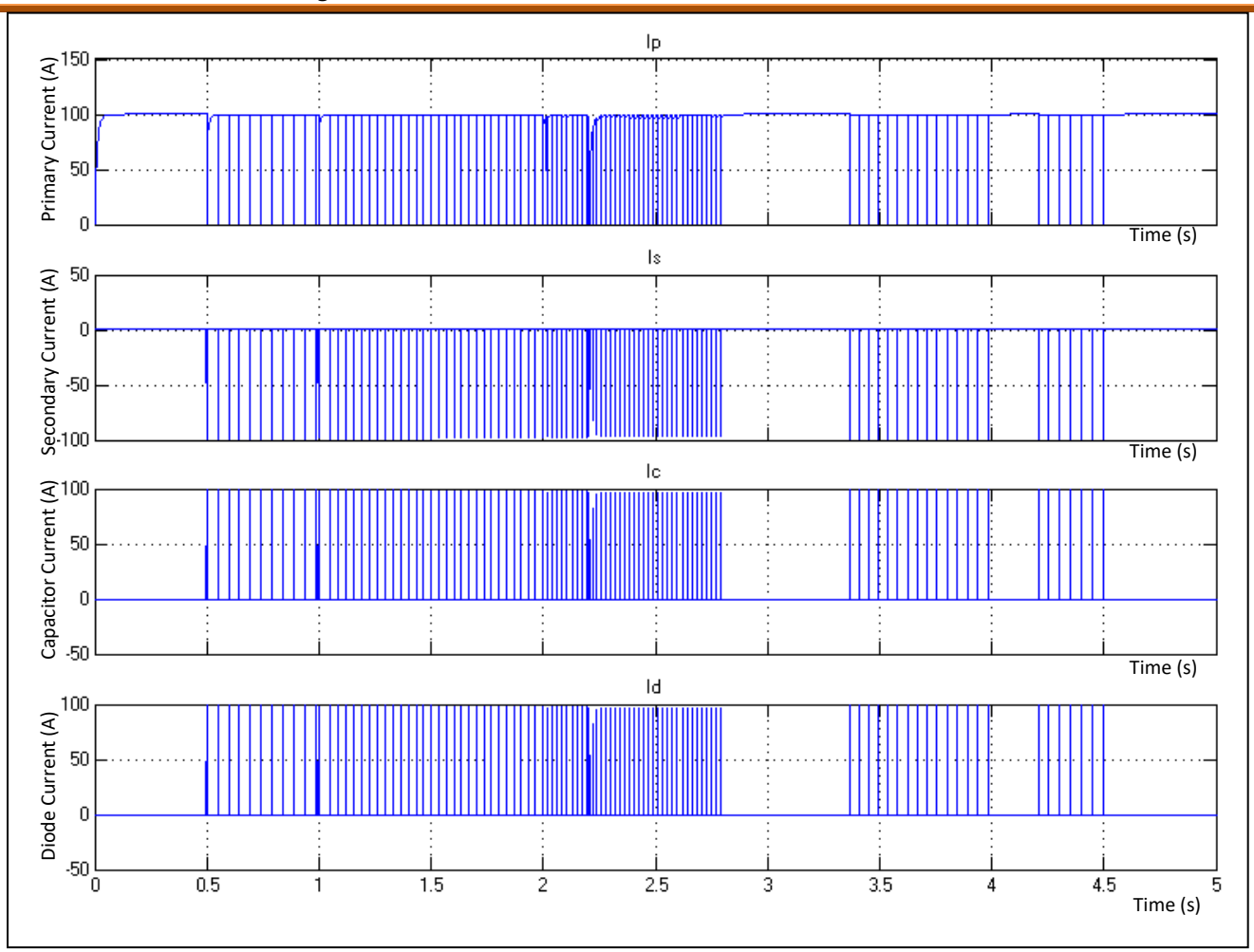

Fig. 9. Fig. 2. Graphs of change of main branch currents (primary, secondary, capacitor and diode current) in flyback converter system according to simulation time.

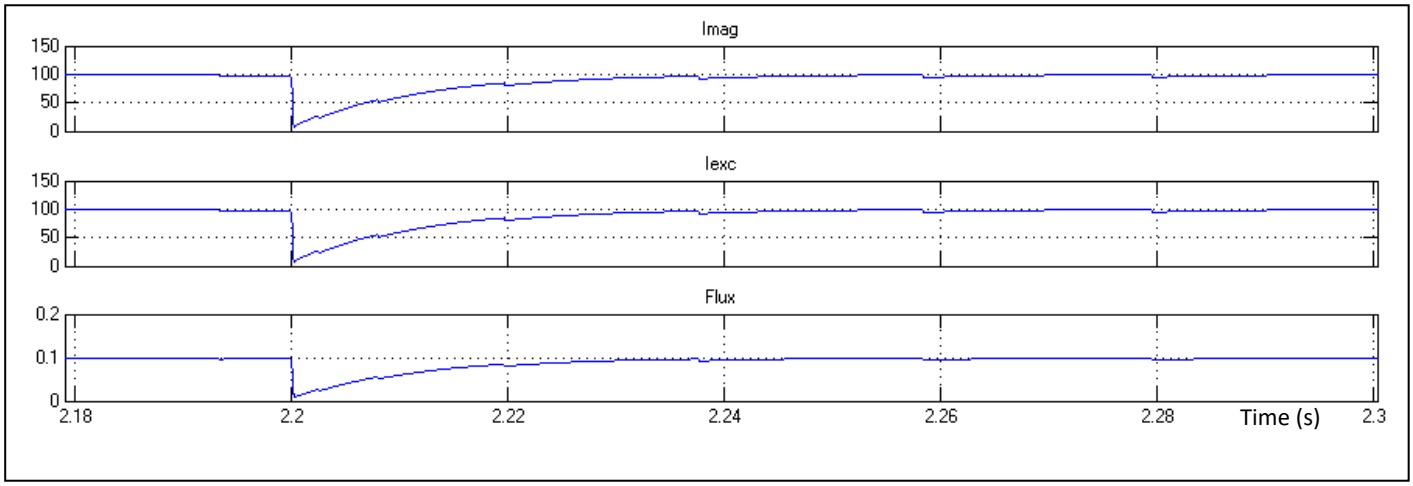

Fig. 10. Detailed changes of magnetizing current (Imag), excitation current (Iexc), magnetic leakage flux (Flux) parameters to compensate for the large change in reference between 2.18-2.3 seconds.

In Figure 10, as can be seen especially in Figure 7-a), magnetizing current (Imag), excitation current (Iexc), magnetic leakage flux between 2.18-2.3 seconds in order to meet the demand for a sudden rise from 320 Volts to 450 Volts. Detailed changes of (Flux) parameters are given. The system has met this huge demand with a well designed controller with only 10 V input. In Figure 11, some important parameters of the transformer, which is the magnetic coupling element that undertakes the main energy conversion load of the system, are examined. In a) from top to bottom, respectively, the output voltage (V_o), the voltage induced in the primary winding (Uw1), the voltage induced in the secondary winding (Uw2), the magnetizing current (Imag), the excitation current (Iexc), the magnetic leakage flux (Flux) changes are given.

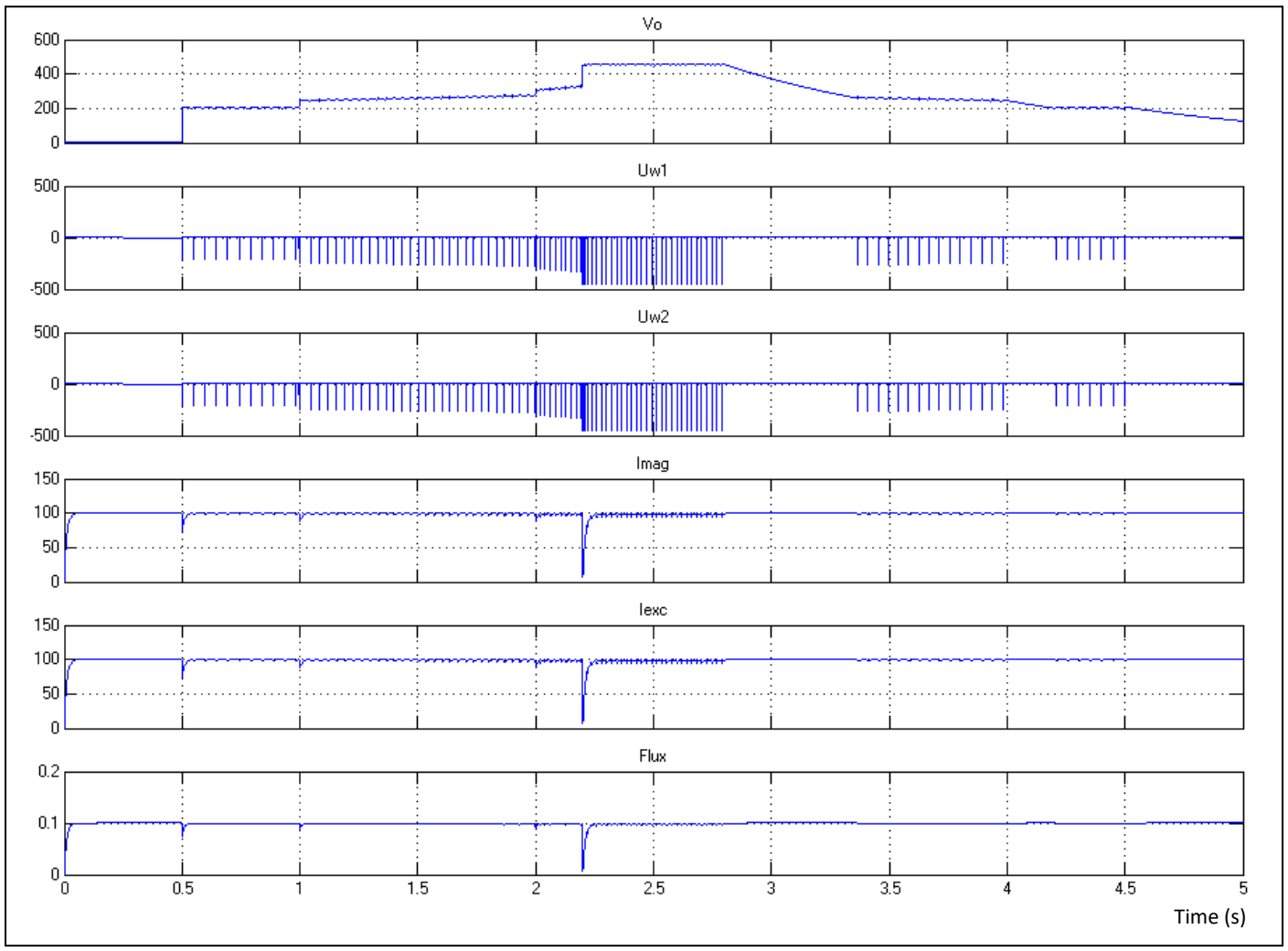

Fig. 11. From top to bottom, respectively, the output voltage (Vo), the voltage induced in the primary winding (Uw1), the voltage induced in the secondary winding (Uw2), the magnetizing current (Imag), the excitation current (Iexc), the magnetic leakage flux (Flux) changes.

5. CONCLUSIONS

In this study, a fuzzy-based control system that can produce the desired voltage with a flyback type DC-DC converter with a small voltage source is designed. The model of the system was analyzed theoretically and created in the MATLAB/Simulink environment. It is thanks to well-designed circuit elements and fuzzy logic-based controller that the demand to produce a voltage of approximately 450 Volts, especially with a voltage of 10 Volts at the input, is met. In accordance with the purpose of the system, very large voltage signals are produced with small DC voltages. Variable instantaneous input references have proven by simulation results that the system works without being affected by transients, that is, without any power interruption, produces the desired voltage, and that the system is stable. Although the system works quite efficiently with this simulation, it needs to be tested for situations other than normal operating conditions under a real load.

6. REFERENCES

[1] Dinçer F. "The Analysis on Photovoltaic Electricity Generation Status, Potential and Policies of the Leading Countries in Solar Energy". Renewable and Sustainable Energy Reviews, 15(1), 713-720, 2011.

[2] Zenk, H. (2018). Investigation of Energy Efficiency in Turkey. Annals of the Faculty of Engineering Hunedoara, 16(1), 93-96.

[3] Zenk, H. (2018). Low Cost Provides of the Energy Needs of Plateau Houses by Using Photovoltaic Systems. Turkish Journal of Agriculture-Food Science and Technology, 6(12), 1768-1774.

[4] https://www.iea.org/fuels-and-technologies/renewables.

[5] Güner, F., Başer, V., & Zenk, H. (2021). Evaluation of offshore wind power plant sustainability: a case study of Sinop/Gerze, Turkey. International Journal of Global Warming, 23(4), 370-384.

[6] Demir, E., Zenk, H., & Başer, V. (2021). Technical Aspects of Analysis of Offshore Wind Power Plant Installation in Turkey. In 2nd International Conference on Agriculture, Technology, Engineering andSciences (ICATES 2019), pp. 529-535.

[7] Zenk, H. (2019). Comparison of the performance of photovoltaic power generation-consumption system with push-pull converter under the effect of five different types of controllers. International Journal of Photoenergy, 2019.

[8] Zenk, H. & Akpinar, A. S. (2013). Solar Power Generation Potentials of The Houses in Turkey. International Conference on Environmental Science and Technology (ICOEST 2013).

[9] Guner, F., & Zenk, H. (2020). Experimental, Numerical and Application Analysis of Hydrokinetic Turbine Performance with Fixed Rotating Blades. Energies, 13(3), 766.

[10] Guner, F., & Zenk, H. (2019). Hydrokinetic Energy Conversion Systems in Turkey an Experimental Analysis. In 2nd International Conference on Agriculture, Technology, Engineering and Sciences (ICATES 2019), pp. 589-597.

[11] Şenol, H., & Zenk, H. (2020). Determination of the biogas potential in cities with hazelnut production and examination of potential energy savings in Turkey. Fuel, 270, 117577.

[12] Zenk, H. (2019). The Electric Energy Potential of Samsun City from Animal Manure. European Journal of Science and Technology, (17), 1307-1312.

[13] Şenol, H., & Zenk, H. (2019). Biogas Production and Current Purification Methods. In 2nd International Conference on Agriculture, Technology, Engineering and Sciences (ICATES 2019), pp. 515-521.

[14] Dickson, M. H., & Fanelli, M. (2013). Geothermal energy: utilization and technology. Routledge.

[15] Zenk, H. (2016). In push-pull converter output voltage stability comparison with using fuzzy logic, PI and PID controllers. International Journal of Engineering Research and Management (IJERM), 3(12), 1-6.

[16] Zenk H., Kara A.,Güney M. S, Güner F., & Zenk O. (2018). PMDC Motor Speed Control With Fuzzy Logic Controlled Zeta Converter. 4rd International Conference on Engineering and Natural Sciences (ICENS 2018), 4(1), 502-502.

[17] Zenk, H. (2019). Effective Control of the Developmental Current of a Serial DC Motor with a Fuzzy Tuned-PI Controller Zeta Converter. Karadeniz Fen Bilimleri Dergisi, 9(1), 196-211.

[18] Zenk, H. (2016). A Comparative Application of Performance of the SEPIC Converter Using PI, PID and Fuzzy Logic Controllers for PMDC Motor Speed Analysis. Journal of Multidisciplinary Engineering Science Studies (JMESS), 2(12), 1226-1231.

[19] Zenk, H., & Akpinar, A. S. (2014). Dynamic Performance Comparison of Cúk Converter with DC Motor Driving and Using PI, PID, Fuzzy Logic Types Controllers. Universal Journal of Electrical and Electronic Engineering, 2(2), 90-96.

[20] Zenk, H. (2018). Comparison of Output Parameters of Two-Phase Interleaved Buck Converter Using Different Type Control Methods. Journal of Multidisciplinary Engineering Science Studies (JMESS), 4(11), 2271-2276.

[21] Zenk, H. (2017). High Performance DC Converter Designs With Controlled By A Simulink Software For Electric Motors. International Journal of Engineering and Information Systems (IJEAIS), 1(10), 58-66.

[22] Zenk, H. (2018). Comparison of Electrical Performances of Power Electronics Switches and an Effective Switch Selection Algorithm. Acta Physica Polonica A, 133(4), 897-901.

[23] Zenk, H. (2018). An Effective Flyback Converter Design for PMDC Motor Control. Karadeniz Fen Bilimleri Dergisi, 8(2), 207-215.

[24] Zenk, H. (2020). Comparison of Voltage Stability of Photovoltaic Power Source Dual Structure Flyback Converter with Fuzzy-Tuned PI and Fractional PID Type Controllers. The Black Sea Journal of Sciences, 10(2), 443-465.

[25] Zenk, H., & Altaş, İ. H. (2010). Farklı Kural Tabanlı Bulanık Mantık Denetleyicilerle DA Motorunu Denetlerken Performanslarının Kıyaslanması. TOK, 10, 21-23.

[26] Akyazı, Ö., Zenk, H., & Akpınar, A. S. (2011). Farklı Bulanık Üyelik Fonksiyonları Kullanarak Sürekli Mıknatıslı DA Motorunun Hız Denetiminin Gerçeklenmesi. In 6th International Advanced Technologies Symposium (IATS'11) (pp. 16-18).

[27] Zenk, H., & Akpınar, A. S. (2012). Multi zone power systems load-frequency stability using fuzzy logic controllers. JECE, Journal of Electrical and Control, 2(6), 49-54.

[28] Zenk, H., Zenk, O., & Akpinar, A. S. (2011). Two different power control system load-frequency analysis using fuzzy logic controller. In 2011 International Symposium on Innovations in Intelligent Systems and Applications (pp. 465-469). IEEE.

[29] Zenk, H., & Akpinar, A. S. (2013). PI, PID and fuzzy logic controlled SSSC connected to a power transmission line, voltage control performance comparison. In 4th International Conference on Power Engineering, Energy and Electrical Drives (pp. 1493-1497). IEEE.

[30] Zenk, H., & Altinkok, A. (2017). Output Voltage Control of PI And Fuzzy Logic Based Zeta Converter. IOSR Journal of Electrical and Electronics Engineering (IOSR-JEEE), 12(6), 63-70.

[31] Zenk, H., & Zenk, O. (2017). The Eight Zones Power Systems Load-frequency Stability Using Different Type Controllers. DEStech Transactions on Environment, Energy and Earth Sciences, (PEEM2016), pp. 63-68.